

## Size-Controlled Submicrometer Hollow Spheres Constituted of ZnO Nanoplates from Layered Zinc Hydroxide

Makoto Moriya, Kyohei Yoshikawa, Wataru Sakamoto, and Toshinobu Yogo\*

*Ecotopia Science Institute, Nagoya University, Nagoya 464-8603, Japan*

Received May 5, 2009

A layered zinc compound is afforded by the heating of zinc acetate dihydrate with mandelic acid in dibenzyl ether. Thermolysis of the layered compound results in the formation of hollow spheres constructed from plate-like ZnO nanocrystals (NCs) in high yield. Size-controlled hollow spheres with a 690 nm diameter (size variation = 6.0%) are obtained by thermal treatment at 300 °C for 15 h. In this reaction, the mandelate moiety plays important roles not only in morphology control of ZnO NCs but also for the formation of hollow structures constituted of ZnO nanoplates.

### Introduction

Nanocrystals (NCs) that possess hollow structures have attracted considerable attention owing to their unique structural, optical, and electrical properties.<sup>1–18</sup> Therefore, applications exploiting their highly specific surface area and large cavities, such as electrodes for dye-sensitized solar cells and carriers for drug delivery systems, are being studied in detail. Zinc oxide (ZnO) is one of the most suitable materials for these purposes since it is nontoxic, cheap, and is a wide-bandgap (3.37 eV) semiconducting material. In general, hollow structures consisting of ZnO NCs are fabricated in one of three ways: the “template method”,<sup>8–12</sup> the “emulsion system”,<sup>13–15</sup> or the “Kirkendall effect” mechanisms.<sup>16–18</sup> In the “template method”, the surfaces of template spheres made of polymer or silica are covered with precursors for ZnO and then

transformed into ZnO by a thermolysis or hydrolysis reaction and the subsequent removal of the templates by calcination or dissolution with solvents. The “emulsion system” yields the hollow structure of ZnO NCs in the reverse micelle structure which behaves like a soft template. The “Kirkendall effect” is a well-known physical phenomenon which involves the different diffusivities among different atomic species.

The reaction mechanism tends to affect the size and morphology of ZnO NCs that compose hollow structures. Since the crystal structure of ZnO is the Wurtzite form which has *c*-axial anisotropy, the emulsion system and Kirkendall effect mechanisms often result in the formation of the hollow spheres as ordered aggregates of ZnO nanorods.<sup>8–12</sup> Although sophisticated processes have been reported, it is still important to develop new routes to synthesize hollow structures since the chemical and physical properties of assembled nanocrystalline materials are often governed by the size, morphology, and ordered arrangement of NCs.

We have investigated the preparation of size- and morphology-controlled metal oxide NCs using mandelic acid (a biobased hydroxyl carboxylic acid) because the strong interaction between mandelic acid and metal centers is expected owing to their large dipole moment and chelate effect.<sup>19</sup> Size and morphology control over NCs is generally achieved by the use of surfactant molecules during synthesis via solution processes such as hydrothermal reaction and thermal decomposition reaction.<sup>20–24</sup> The molecular

\*To whom correspondence should be addressed. E-mail: yogo@esi.nagoya-u.ac.jp. Fax: +81-52-789-2121.

- (1) Caruso, F.; Caruso, R. A.; Möhwald, H. *Science* **1998**, *282*, 1111.
- (2) Caruso, F.; Spasova, M.; Susha, A.; Giersig, M.; Caruso, R. A. *Chem. Mater.* **2001**, *13*, 109.
- (3) Yang, H. G.; Zeng, H. C. *J. Phys. Chem. B* **2004**, *108*, 3492.
- (4) Yin, Y.; Rioux, R. M.; Erdonmez, C. K.; Hughes, S.; Somorjai, G. A.; Alivisatos, A. P. *Science* **2004**, *304*, 711.
- (5) Peng, Q.; Dong, Y.; Li, Y. *Angew. Chem., Int. Ed.* **2003**, *42*, 3027.
- (6) Sun, Y.; Xia, Y. *Science* **2002**, *298*, 2176.
- (7) Sun, Y.; Mayers, B.; Xia, Y. *Adv. Mater.* **2003**, *15*, 641.
- (8) Mo, M.; Yu, J. C.; Zhang, L.; Li, S.-K. A. *Adv. Mater.* **2005**, *17*, 756.
- (9) Izaki, M.; Watanabe, M.; Aritomo, H.; Yamaguchi, I.; Asahina, S.; Shinagawa, T.; Chigane, M.; Inaba, M.; Tasaka, A. *Cryst. Growth Des.* **2008**, *8*, 1418.
- (10) Gao, S.; Zhang, H.; Wang, X.; Deng, R.; Sun, D.; Zheng, G. *J. Phys. Chem. B* **2006**, *110*, 15847.
- (11) Deng, Z.; Chen, M.; Gu, G.; Wu, L. *J. Phys. Chem. B* **2008**, *112*, 16.
- (12) Wang, X.; Hu, P.; Fangli, Y.; Yu, L. *J. Phys. Chem. C* **2007**, *111*, 6706.
- (13) Cong, H.-P.; Yu, S.-H. *Adv. Funct. Mater.* **2007**, *17*, 1814.
- (14) Liu, B.; Zeng, H. C. *Chem. Mater.* **2007**, *19*, 5824.
- (15) Yao, K. X.; Zeng, H. C. *J. Chem. Phys. B* **2006**, *110*, 14736.
- (16) Liu, B.; Zeng, H. C. *J. Am. Chem. Soc.* **2004**, *126*, 16744.
- (17) Shen, G.; Bando, Y.; Lee, C.-J. *J. Phys. Chem. B* **2005**, *109*, 10578.
- (18) Chen, Z.; Gao, L. *Cryst. Growth Des.* **2008**, *8*, 460.

- (19) Moriya, M.; Ito, M.; Sakamoto, W.; Yogo, T. *Cryst. Growth Des.* **2009**, *9*, 1889.
- (20) Burda, C.; Chen, X.; Narayanan, R.; El-Sayed, M. A. *Chem. Rev.* **2005**, *105*, 1025.
- (21) Jun, Y.-W.; Choi, J.-S.; Cheon, J. *Angew. Chem., Int. Ed.* **2006**, *45*, 3414.
- (22) Cushing, B. L.; Kolesnichenko, V. L.; O'Connor, C. J. *Chem. Rev.* **2004**, *104*, 3893.
- (23) Yin, Y.; Alivisatos, A. P. *Nature* **2005**, *437*, 664.
- (24) Pileni, M.-P. *Nat. Mater.* **2003**, *2*, 145.

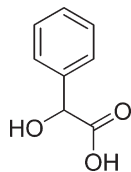


Figure 1. Molecular structure of mandelic acid.

structure, concentration, and molar ratio of the surfactants play an important role in the size and shape of obtained NCs, as well as other reaction conditions such as solvent, reaction temperature and time, and heating rate. However, it is often difficult to obtain a completely reproducible result regarding these reactions since many factors can affect the size and shape of NCs and details of the crystal growth mechanism are not obvious.<sup>25</sup>

In this study, we have attempted to control the size and shape of ZnO NCs via the use of ordered arrays of zinc ions. These compounds will be transformed into the ZnO NCs having the characteristic morphology reflecting the two-dimensional array of zinc atoms. We have selected a layered zinc hydroxide,  $Zn(OH)_n(X)_{2-n}$  ( $X$  = anionic group,  $n = 0-2$ ), for this reason. Because the layered structures comprise two-dimensional arrays of zinc atoms and bridged hydroxyl ligands, they are a suitable precursor for the synthesis of ZnO NCs with two-dimensional morphology and the construction of their hierarchical arrangement.<sup>26-40</sup> We investigated the reaction of zinc acetate with mandelic acid (Figure 1), and interestingly, the reaction resulted in the formation of the stacks of layered zinc hydroxide followed by the formation of hollow spheres constructed from ZnO nanoplates. We herein report the details of this reaction and the resultant method for the formation of hollow spheres induced by microbubble evolution.

## Experimental Section

Zinc acetate dihydrate (98.5%, Hayashi Pure Chemical), DL-mandelic acid (99%, Tokyo Chemical Industry), and dibenzyl ether (95%, Tokyo Chemical Industry) were used as received. The representative procedure for the synthesis

was as follows: mandelic acid (0.25 mmol), zinc acetate (1.25 mmol), and dibenzyl ether (50 mL) were charged in a round-bottom flask. The reaction flask was degassed, and the temperature was raised at a rate of 5 °C/min to 160 °C. Then, 1 atm of nitrogen was charged into the flask, and additional heating was performed to desired temperature at a rate of 5 °C/min. The solution was refluxed for the desired time with vigorous magnetic stirring. The solution turned white and turbid. After the flask was cooled to room temperature, 50 mL of methanol was added to the mixture to give the precipitate, followed by centrifugation (3500 rpm) and decantation. Then, the precipitates were washed with hexane and methanol. This washing process was repeated several times. Finally, the separated precipitates were dried under reduced pressure at 100 °C to yield products as white powder. In the synthesis of **300-15**, 97.1 mg of ZnO NCs was obtained (95%) from 274.8 mg of  $Zn(OAc)_2 \cdot 2H_2O$ .

The products were analyzed by X-ray diffraction (Rigaku, RINT 2500 diffractometer) using Cu K $\alpha$  radiation with a monochromator. Transmission electron microscopy (TEM) images and selected area electron diffraction (SAED) patterns were taken on a HITACHI, H-800 electron microscope at 200 kV. Field-emission scanning electron microscopy (SEM) images were taken on a JEOL, JSM-6330 electron microscope at 15 kV. Thermogravimetry-differential thermal analysis (TG-DTA) was performed with Rigaku, Thermo plus EVO TG8120 with a heating rate of 10 °C/min in O<sub>2</sub> using Al<sub>2</sub>O<sub>3</sub> as a reference. IR spectra were measured with a Nicolet, Nexus 470 FT-IR spectrometer. Photoluminescence analysis with a Perkin-Elmer, LS 50B was performed on a chloroform suspension of ZnO NCs directly at room temperature using 300 nm as an excitation wavelength.

## Result and Discussion

The literature demonstrates that layered zinc compounds have been obtained by thermal treatment of zinc acetate or zinc hydroxide in the presence of carboxylic acid.<sup>26-40</sup> Taking these results into account, we attempted to create these compounds by heating zinc acetate dihydrate with mandelic acid in dibenzyl ether. The molar ratio between zinc acetate and mandelic acid was fixed at 1:0.2 because the formula of layered zinc hydroxides with an acetate group is generally represented as  $Zn_5(OH)_8(CH_3COO)_2$  and both the hydroxyl and the carboxyl groups of mandelic acid would coordinate to zinc center. Although mandelic acid has a chiral carbon, we used a racemic mixture of DL-mandelic acid in this study since the racemization between D- and L-mandelic acid easily takes place under thermal conditions.<sup>41</sup> The reaction was carried out at a heating rate of 5 °C/min to 160 °C under reduced pressure to remove volatile components. Next, nitrogen was introduced into the flask at 1 atm followed by subsequent heating to 200, 250, and 300 °C at the rate of 5 °C/min, and the temperature was maintained for the desired amount of time. After cooling, methanol was added to give the products, **T-m** ( $T$  = temperature (200, 250, or 300 °C),  $m$  = heating time (h)), as a white powder. Then, the powder was separated by centrifuging, washed with methanol and hexane, and dried under reduced pressure at 100 °C. In the case of **300-15**, ZnO NCs were obtained at a yield of 95% on the basis of molar ratio of  $Zn(CH_3COO)_2 \cdot 2H_2O$ .

X-ray diffraction (XRD) patterns of **200-0** and **250-0** gave strong diffraction peaks at regular intervals between  $2\theta = 2$  to  $10^\circ$ , indicating the presence of layered zinc hydroxides

(25) Turgeman, R.; Tirosh, S.; Gedanken, A. *Chem. Eur. J.* **2004**, *10*, 1845.

(26) Song, R.-Q.; Xu, A.-W.; Deng, B.; Li, Q.; Chen, G.-Y. *Adv. Funct. Mater.* **2007**, *17*, 296.

(27) Zhang, W.; Yanagisawa, K. *Chem. Mater.* **2007**, *19*, 2329.

(28) Liu, B.; Yu, S.-H.; Zhang, F.; Li, L.; Zhang, Q.; Ren, L.; Jiang, K. *J. Phys. Chem. B* **2004**, *108*, 4338.

(29) Liang, J.; Liu, J.; Xie, Q.; Bai, S.; Yu, W.; Qian, Y. *J. Phys. Chem. B* **2005**, *109*, 9463.

(30) Zhao, F.; Lin, W.; Wu, M.; Xu, N.; Yang, X.; Tian, Z. R.; Su, Q. *Inorg. Chem.* **2006**, *45*, 3256.

(31) Arizaga, G. G. C.; Satyanarayana, K. G.; Wypych, F. *Solid State Ionics* **2007**, *178*, 1143.

(32) Liang, C.; Shimizu, Y.; Masuda, M.; Sasaki, T.; Koshizaki, N. *Chem. Mater.* **2004**, *16*, 963.

(33) Rocca, E.; Caillet, C.; Mesbah, A.; Francois, M.; Steinmetz, J. *Chem. Mater.* **2006**, *18*, 6186.

(34) Xing, L.-L.; Yuan, B.; Hu, S.-X.; Zhang, Y.-D.; Lu, Y.; Mai, Z.-H.; Li, M. *J. Phys. Chem. C* **2008**, *112*, 3800.

(35) Kasai, A.; Fujihara, S. *Inorg. Chem.* **2006**, *45*, 415.

(36) Ogata, S.; Tagaya, H.; Karasu, M.; Kadokawa, J.-I. *J. Mater. Chem.* **2000**, *10*, 321.

(37) Miao, J.; Xue, M.; Itoh, H.; Feng, Q. *J. Mater. Chem.* **2006**, *16*, 474.

(38) Ogata, S.; Tasaka, Y.; Tagaya, H.; Kadokawa, J.-I.; Chiba, K. *Chem. Lett.* **1998**, *27*, 237.

(39) Aisawa, S.; Ishida, E.; Takahashi, S.; Hirahara, H.; Narita, E. *Chem. Lett.* **2005**, *34*, 630.

(40) Kuo, C. L.; Kuo, T. J.; Huang, M. H. *J. Phys. Chem. B* **2005**, *109*, 20115.

(41) Liu, T.; Simmons, T. L.; Bohnsack, D. A.; Mackay, M. E.; Smith, M. R., III; Baker, G. L. *Macromolecules* **2007**, *40*, 6040.

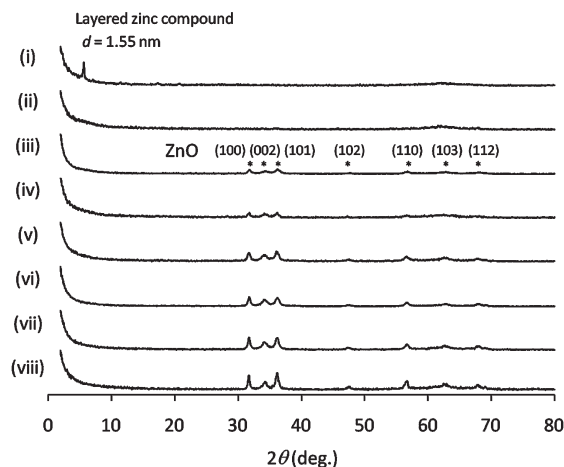


**Figure 2.** Time dependent change of XRD patterns of the zinc compounds obtained at 200 °C. (i) 0 h. (ii) 1 h. (iii) 2 h. (iv) 3 h. (v) 5 h. (vi) 10 h. (vii) 15 h. (viii) 39 h.

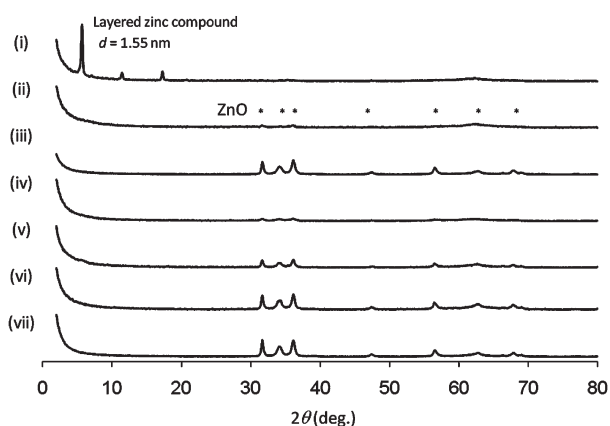


**Figure 3.** Time dependent change of XRD patterns of the zinc compounds obtained at 250 (i, ii, and iii) and 300 °C (iv, v, and vi). (i) 0 h. (ii) 1 h. (iii) 5 h. (iv) 0 h. (v) 1 h. (vi) 5 h. (vii) 15 h.

(Figure 2, 3 and Supporting Information, Figure S1). Both the interlayer distances of **200-0** and **250-0** were calculated to be 1.55 nm using Bragg's law, a value which is comparable to that of layered zinc benzoate,  $\text{Zn}_5(\text{OH})_8(\text{C}_6\text{H}_5\text{COO})_2$ .<sup>37</sup> The obtained 1.55 nm layered phase shows main diffraction peaks with *d*-values of 1.55, 0.78, and 0.52 nm. These results strongly suggest the formation of a layered zinc hydroxide containing mandelate moieties. Heating at 200 °C for 1 h resulted in the disappearance of the layered zinc compound, and thermal treatment exceeding 2 h led to the formation of ZnO NCs (Figure 2(iii)). Compared to the intensity ratio among the peaks attributable to (100), (002), and (101) in the XRD pattern of bulk ZnO (JCPDS 361451), the intensity of the (100) and (002) reflections to that of (101) reflection of the obtained ZnO NCs increases in these reactions. The time dependent change of the crystallite size was calculated from the Scherrer equation using the reflections observed at  $2\theta = 32$  and  $36^\circ$  (Figure 4). It shows that the crystal growth rate along (100) and (002) is constant at 2:1 in the early stage of the reaction, and it reaches a plateau after 10 h of thermal treatment at 200 °C. At the plateau, the crystallite sizes along (100) and (002) were estimated to be 20 and 10 nm, respectively. This indicates that the layered zinc hydroxide successfully suppresses the crystal growth toward the *c*-axis of the ZnO NCs in this reaction. Also,

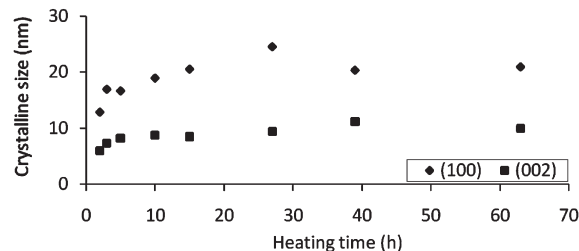


**Figure 4.** Time dependent change of the crystallite sizes of ZnO nanoplates at 200 °C along (100) and (002).

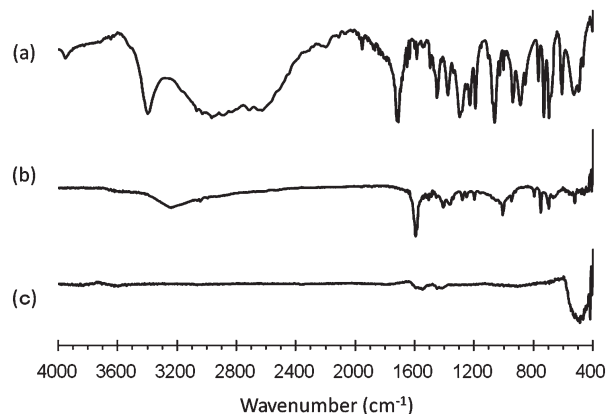


**Figure 5.** IR spectra of the starting material and zinc compounds. (a) mandelic acid, (b) **200-0**, (c) **300-15**.

higher reaction temperature induces the rapid formation of ZnO NCs.

IR spectra of the products and mandelic acid are shown in Figure 5. The spectrum of mandelic acid shows peaks from a hydroxyl group at  $3392\text{ cm}^{-1}$  and a carboxylic acid moiety at  $1711\text{ cm}^{-1}$ . The absorption band observed at  $1030\text{ cm}^{-1}$  is assignable to the stretching vibration of the  $\text{C}_{\text{benzyl}}\text{--O}_{\text{hydroxyl}}$  bond. The broaden peak observed from  $2621\text{ cm}^{-1}$  to  $3028\text{ cm}^{-1}$  can be attributed to the stretching vibration of the oxygen–hydrogen bond of the carboxylic group. On the other hand, in the spectrum of **200-0**, the carboxylic acid peak is not present and new peaks attributed to a carboxylate group were observed at  $1358$  and  $1593\text{ cm}^{-1}$ .<sup>42</sup> The layered compound, **200-0**, shows a peak from a hydroxyl group at  $3221\text{ cm}^{-1}$ . The difference in the wavenumber of  $\nu(\text{O--H})$  between mandelic acid and the layered zinc compound should mean the hydroxyl group of the layered zinc compound has attached to the zinc centers while that of mandelic acid forms a carbon–oxygen bond. The layered zinc compound, **200-0**, gave strong absorptions at  $1004$  and  $1063\text{ cm}^{-1}$  due to the stretching vibration of carbon–oxygen bond of mandelate ligands and benzyl ether, respectively.<sup>42</sup> The absorptions around  $1402$  and  $1593\text{ cm}^{-1}$  are assignable to  $\nu(\text{C}=\text{C}_{\text{aromatic}})$  of mandelate and benzyl ether. Furthermore, the peaks at  $692$  and  $752\text{ cm}^{-1}$  indicate a bending vibration of aromatic carbon–hydrogen bonds, as well as a stretching vibration at  $3039\text{ cm}^{-1}$ .<sup>42</sup> These results indicate that the obtained layered zinc compound contains hydroxyl, mandelate groups and benzyl ether. In the spectrum of ZnO NCs, **300-15**, a strong and broad peak based on  $\nu(\text{Zn--O})$  was found at  $457\text{ cm}^{-1}$ , and the weak peaks of the

(42) Silverstein, R. M.; Webster, F. X. *Spectrometric Identification of Organic Compounds*; 6th ed.; Wiley: New York, 1998.

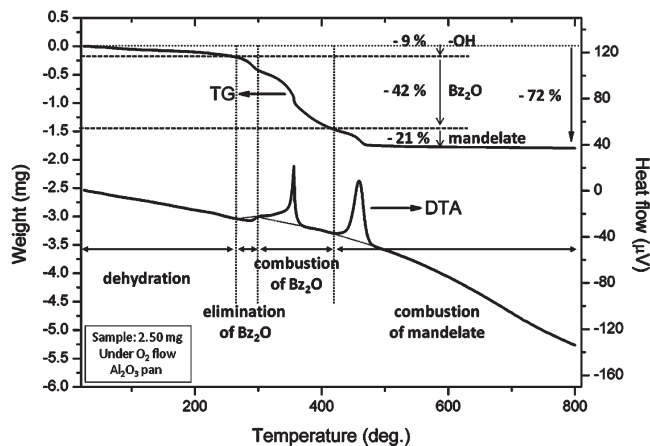


Figure 6. TG-DTA curves of 200-0.

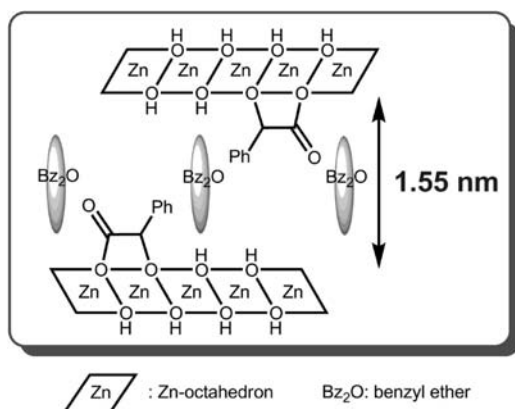


Figure 7. Plausible structure model for the layered zinc compound.

$\nu(\text{COO}^-)$  and  $\nu(\text{C}=\text{C}_{\text{aromatic}})$  were observed from 1400 to 1600  $\text{cm}^{-1}$ . This indicates that the surface of the obtained ZnO NCs is covered with mandelate ligands.

TG-DTA analyses indicate the difference in the ratio of organic moiety between the layered zinc compound, **200-0**, and ZnO NCs, **300-15** (Figure 6 and Supporting Information, Figure S2). In this measurement, the weight loss for **200-0** and **300-15** induced by the combustion of organic moieties was analyzed and found to be 72 wt % and 15 wt %, respectively, and the residues of both samples were confirmed as zinc oxide from their XRD patterns. In the DTA curve of **200-0**, one endothermic peak and two exothermic peaks were observed. In the early stage of the analysis, the weight loss attributable to the dehydration from hydroxyl moiety at zinc center was confirmed. The weight loss ratio for the dehydration reaction was calculated to be 9%, and the endothermic peak at 286 °C and the exothermic peak at 356 °C were detected. These peaks were attributed to the elimination of guest molecules (benzyl ether, in this case) from the interlayer spaces and their combustion, respectively. The peak at 459 °C was attributed to the combustion of mandelate groups at the surface of the layered compound. Conversely, the DTA curve of ZnO NCs, **300-15**, showed only one peak at 460 °C, which was assigned to the combustion of the mandelate moiety. The weight loss ratio of **200-0** for benzyl ether and the mandelate group were estimated to be 42 and 21%, respectively.

These results indicate that the formula for the layered zinc compound can be represented as  $\text{Zn}(\text{OH})_{1.6}(\text{C}_6\text{H}_5\text{CH}(\text{OH})\text{COO})_{0.2} \cdot (\text{C}_6\text{H}_5\text{CH}_2\text{OCH}_2\text{C}_6\text{H}_5)_{0.6}$ . The  $d$ -values of single

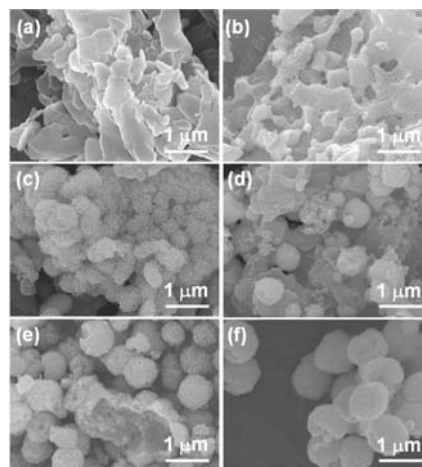


Figure 8. SEM images of the layered zinc compounds and ZnO NCs. (a) 200-0. (b) 200-1. (c) 200-2. (d) 200-5. (e) 200-15. (f) 250-63.

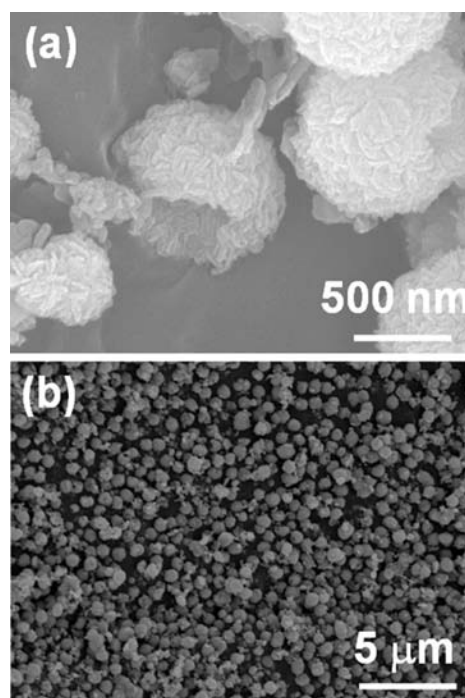
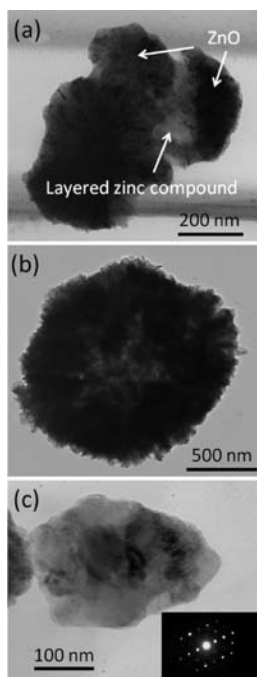


Figure 9. SEM images of the hollow spheres. (a) 250-63, (b) 300-15.

layer zinc hydroxide with a benzoate group are reported to be 1.32 and 1.47 nm, while that of the triple-decker zinc hydroxide containing benzoate is 1.93 nm.<sup>37</sup> Since the interlayer distance of the obtained compound is similar to that of single layered zinc hydroxide, the zinc ions in the obtained layered compound would be arrayed in a single layer structure rather than a triple-decker type structure. Therefore the layered zinc compound should be constructed from zinc ions having a single layer two-dimensional array. The two-dimensional arrangement of the zinc ions would be maintained by the bridged hydroxyl and mandelate groups as shown in Figure 7.

SEM images of the products are shown in Figure 8. The formation of layered structures of zinc mandelate nanosheets was confirmed in the image of **200-0** (Figure 8a). The layered structures gradually decomposed while foam structures were observed at the surface as the reaction time increased

(Figure 8b and 8c). Heating beyond 5 h resulted in the formation of spherical and hemispherical aggregations of ZnO NCs (Figure 8d and 8e). The image of **250-63** (Figure 8f) and its magnified image (Figure 9a) indicate that higher reaction temperatures and longer reaction times lead to the formation of spheres with cavities and hollow structures which are constructed via the stacking of ZnO nanoplates. Both the inner and outer surfaces of the hollow spheres were not smooth but rather seemed to be stone-wall-like. The thickness of the nanoplates was estimated to be at approximately 10 nm. Increasing the temperature to 300 °C for 15 h resulted in the formation of size-controlled



**Figure 10.** TEM images of the products. (a) Layered zinc compound and hollow hemisphere, **200-3**. (b) Hollow sphere, **300-15**. (c) ZnO nanoplate removed from a hollow sphere. Inset is the selected area electron diffraction (SAED) pattern, **200-2**.

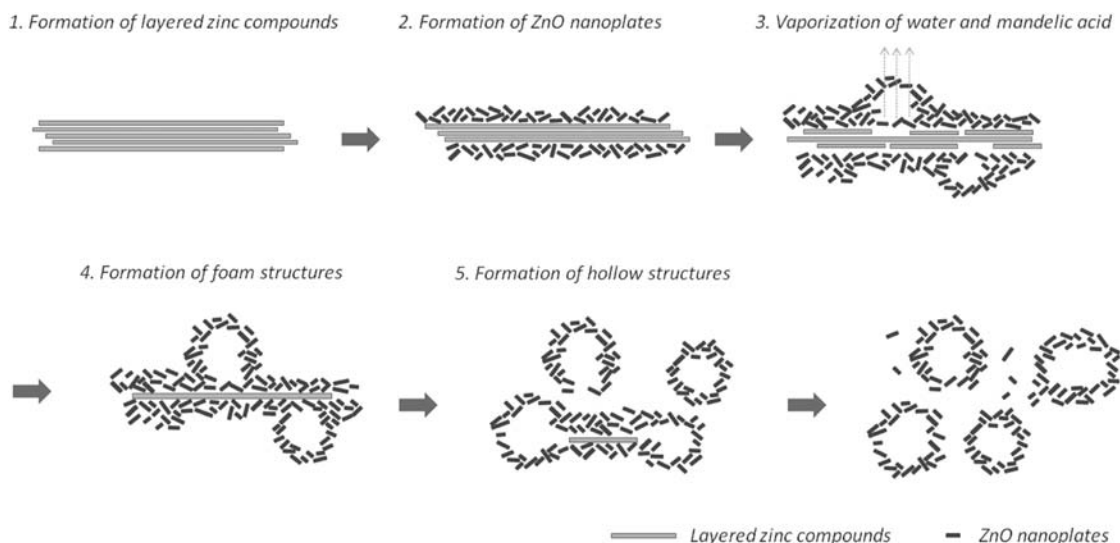
hollow spheres 690 nm in diameter (size variation = 6.0%) (Figure 9b).

Formation of hollow spheres constructed from ZnO nanoplates was also confirmed from TEM images (Figure 10). In the early stages of the reaction, hollow hemispheres formed from the layered zinc compound (Figure 10a). In the image presented in Figure 10b, the hollow sphere composed from ZnO nanoplates is shown. Because the center area of the sphere is brighter than the edge area in this image, the cavity should be located at the center of the sphere. The ZnO nanoplate, which was assumed to have been removed from the hollow spheres during the sample preparation process for TEM analysis, is depicted in Figure 10c. The selected area electron diffraction (SAED) pattern of the ZnO nanoplate shows the projection image corresponding to the [001] zone axis. These results indicate that the use of zinc mandelate nanosheets plays an important role in the selective inhibition of crystal growth along the *c*-axis of ZnO and the construction of ordered assembly of NCs.

The plausible reaction mechanism for the formation of hollow spheres is described in Scheme 1. The reaction of zinc acetate with mandelic acid initially yields layered zinc mandelate nanosheets. Further heating induces thermal decomposition of the nanosheets at the surface to give thin, small flakes of ZnO NCs. This reaction leads to the formation of a core-shell structure where the core is constituted of zinc mandelate and the shell is constructed from the aggregation of ZnO nanoplates. Next, the thermolysis of the zinc mandelate core covered with the shell structure takes place. Owing to the high reaction temperature, the elimination and vaporization of water proceeds to create microbubbles at the interfaces between the shells of the ZnO NCs aggregates and the core of layered zinc mandelate as well as to initiate the transformation of layered zinc mandelate into ZnO NCs. Therefore, the foam structures would be formed at the surface of the core-shell structure. As the reaction proceeded, the surface swelling and aggregation of ZnO nanoplates increased in size and ultimately yielded hollow spheres.

Some reports have mentioned that hollow structures constructed from nanorods are stable under severe conditions such as the ultrasonic irradiation.<sup>8</sup> On the contrary,

**Scheme 1.** Plausible Reaction Mechanism for the Formation of Hollow Structure from Layered Zinc Compound



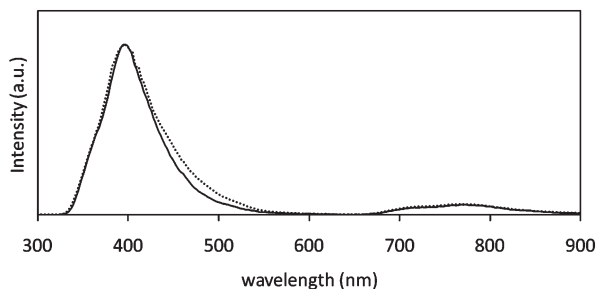


**Figure 11.** PL spectra of ZnO nanoplates obtained at 300 °C for 15 h using mandelic acid (solid line) and hexahydromandelic acid (dotted line).

the hollow structures composed of ZnO nanoplates obtained in this reaction were found to be fragile. The hollow structures collapsed into a dispersion of ZnO nanoplates when heated to 300 °C for 63 h (Supporting Information, Figure S3).

The photoluminescence (PL) spectra of ZnO NCs with an excitation wavelength of 300 nm demonstrated that the emission peak in chloroform was located at 395 nm (Figure 11). Since the emission attributed to the  $\pi$ - $\pi^*$  transient of aromatic rings is often observed in the ultraviolet region, we also attempted to synthesize ZnO NCs using hexahydromandelic acid instead of mandelic acid and heating to 300 °C for 15 h to measure the PL spectrum. The emission peak of the obtained ZnO NCs was also

observed at 395 nm similarly to that of **300-15**. These results indicate that emission at 395 nm corresponds to the near band edge emission of ZnO due to the recombination of excitons.<sup>43</sup>

## Conclusion

In conclusion, we synthesized novel layered zinc carboxylate nanosheets using DL-mandelic acid. These nanosheets were easily transformed into size-controlled submicrometer sized hollow spheres constructed from ZnO nanoplates. The hollow structure was created by microbubble evolution in the core-shell structure. We also discovered that mandelic acid is a useful capping ligand which suppresses the formation of oxygen vacancies as well as serves as a source of zinc mandelate nanosheets and hollow spheres constructed from ZnO nanoplates. PL spectroscopy showed that the hollow spheres have a UV emission peak at 395 nm without visible emission derived from the oxygen vacancy on the surface of ZnO NCs.

**Acknowledgment.** This work was partially supported by The Murata Science Foundation.

**Supporting Information Available:** Magnified image of XRD patterns of the starting material and layered zinc compound, **200-0** and **250-0** (Figure S1). TG-DTA curve of **300-15** (Figure S2). SEM image of **300-63** (Figure S3). This material is available free of charge via the Internet at <http://pubs.acs.org>.

(43) Vanheusden, K.; Warren, W. L.; Seager, C. H.; Tallant, D. R.; Voigt, J. A.; Gnade, B. E. *J. Appl. Phys.* **1996**, *79*, 7983.